Nonlinear dynamics of a loss-switched CO_2 laser

A. M. Samson, S. I. Turovets, V. N. Chizhevskiĭ, and V. V. Churakov

Institute of Physics, Academy of Sciences of Belarus
(Submitted 26 September 1991)
Zh. Eksp. Teor. Fiz. **101**, 1177–1196 (April 1992)

Experiments have been carried out on the nonlinear dynamics of a cw CO_2 laser with acoustooptic loss switching. The results are reported. The resonance structure in the nonlinear response was studied for various relations between the switching frequency and the frequency of relaxation vibrations. The correlation dimension and the entropy are calculated for chaotic regimes on the basis of the experimental data. These calculations are carried out for the one-mode and multimode (in terms of the transverse index) laser regimes. The dynamics of the laser near a period-doubling bifurcation is studied with an additional δ-function Q switching of the resonator by means of an optically controllable absorption in semiconducting elements of the laser. There is a small-signal gain near frequencies which are multiples of half the switching frequency. It is demonstrated that a CO_2 laser with periodic switching can operate as a binary phase flip-flop, a quadratic phase flip-flop, or an amplitude optical flip-flop.

INTRODUCTION

Because of their high stability and relative simplicity, lasers with actively modulated parameters are the most convenient choices for experiments on fundamental aspects of nonlinear dynamics in quantum optics.

The kinetics of single-mode lasers with a wide variety of active media, including most solid state lasers, semiconductor lasers, and certain molecular lasers (e.g., CO_2), obeys two rate equations, for the field and the population inversion of the gain medium. The response of such lasers to a brief and small perturbation is a train of damped relaxation oscillations. This circumstance suggests an analogy with the behavior of a weakly damped oscillator. This fact has been utilized in several previous experimental studies to determine the constants of the rate equations, which are in turn combinations of various physical parameters.[1–3] In order to observe complex processes such as dynamic chaos and accompanying effects, it is necessary to increase the dimensionality of the two-dimensional phase space of the system by at least one. This can be done easily through an active modulation of one parameter of the laser. With a suitable change of variables, the rate equations can be rewritten in a form which is the same as that of the equation of motion of a nonlinear oscillator with a Toda potential, in which the time-dependent part of the modulated parameter serves as a periodic external force. In this modified formulation of the problem, there would necessarily be additional resonances in the system at subharmonics and ultraharmonics of the external force. Consequently, the generation of subharmonics would require the attainment of a threshold. This threshold effect was established in the early theoretical papers on laser dynamics.[4–7] The nonlinear-oscillator model along with the familiar Lorenz model[8] presently occupy central positions in the theory of dynamic chaos. The circumstance that both these models have analogs in laser theory has recently intensified interest in laser dynamics.[9,10]

One of the first experimental results to be offered as evidence for dynamic chaos in lasers that reported by Arecchi *et al.*,[11] who used a CO_2 laser with electrooptic Q switching. They also reported some numerical calculations based on balance equations. They pointed out that the results of these calculations agreed qualitatively with the experimental data. In parallel and independently, chaotic regimes were found in a numerical simulation of the equations of a single-mode solid-state laser with resonator Q switching.[12] Slightly later, regimes of this sort were found experimentally in a traveling-wave Nd:YAG ring laser[13] and also in a mode-locked linear ND:YAG laser with additional low-frequency Q switching.[14]

Further theoretical analysis,[15–17] numerical simulation,[18–21] and analog modeling[22] have drawn a more detailed picture of the onset of nonlinear resonances as a function of the amplitude and frequency of the control signal. They have also drawn a more detailed picture of regions in which various regimes overlap (multistability), of collisions of periodic attractors, and of crises of strange attractors. Comparative analysis of the effectiveness of the switching of various parameters was carried out in Ref. 16, 23, and 24. It was shown in particular that such lasers are considerably more sensitive to switching of the loss coefficient (or the gain) than to modulation of the pump. Many of these results were confirmed experimentally, primarily in CO_2 lasers. This is true in particular in the cases of a modulation of the loss,[25,26] of the resonator length,[27] and of the discharge current.[28] These results have also been confirmed in semiconductor lasers[29] and solid-state lasers with modulated optical pumping based on NdP_5O_{14} crystals[30] and $CoMgF_2$ crystals[31] and optical fibers containing rare earth ions.[3,32]

Several circumstances steer investigators toward CO_2 lasers as objects for studying nonlinear dynamics, as can be seen from the large number of experimental studies using these lasers. One reason is that it is a simple matter to achieve single-mode operation. Another is that the relaxation frequencies lie in the range 50–300 kHz, which is easily realized in modulation. Furthermore, the spontaneous emission of CO_2 lasers is weaker by several orders of magnitude than that in solid-state or semiconductor lasers. When the significant incoherence of the pump is incorporated in the rate equations, the chaos is usually suppressed.[33] In terms of a nonlinear oscillation, the explanation for this result is that the pump increases both the linear and nonlinear parts of the

 0038-5646/92/040628-12$05.00

dissipation coefficient, and it also reduces the pronounced asymmetry of the Toda potential. Both factors lead to an increase in the instability thresholds in the system.[34]

Our purpose in the present study was to pursue experiments on nonlinear dynamic effects in a CO_2 laser with modulated parameters. In contrast with the earlier studies, we used a refractive acoustooptic modulator. We carried out a more detailed study of the resonance structure in the nonlinear response of the laser to a periodic modulation for various relations between the modulation frequency and the frequency of relaxation vibrations. We report results on determining the correlation dimension and the entropy from a chaotic experimental realization in one-mode and multimode regimes. We suggest a combination of sinusoidal modulation and a pulsed modulation of the resonator Q. Such a combination would make it possible to determine the response of the laser to a perturbation near a period-doubling bifurcation. Because of the parametric nature of the period doubling, the laser "amplifies" the spectral components of the perturbation which lie near half the modulation frequency. This amplification can be exploited to increase the sensitivity in in-resonator modulation laser spectroscopy.[35] Although this effect had been predicted previously,[16,36] it has been observed experimentally only in an rf NMR laser.[37]

In general, the presence of several attractors for a given set of parameter values was demonstrated in Refs. 3 and 25–27 by slowly sweeping the control parameter in a sawtooth fashion. The application of a brief pulsed perturbation to the system can in principle cause a rapid switching from one attractor to another— during the pulse itself. Furthermore, by choosing the appropriate amplitude and duration of the pulsed perturbation, one can prepare a system in one of the unstable states. If there is a good signal-to-noise ratio, the system can stay in this state for a fairly long time. In a similar way, it has been demonstrated that it is possible to experimentally determine the unstable part of the S-shaped curve in the region of optical bistability.[38,39] In this paper we are reporting the first experimental study of processes of this sort in a modulated laser.

1. EXPERIMENTAL APPARATUS AND MEASUREMENT PROCEDURE

The experimental apparatus used for this study of dynamics of the lasing in a cw CO_2 laser under Q-switching conditions is shown schematically in Fig. 1.

We used a frequency-stabilized cw CO_2 laser operating on the $10P(22)$ line. The long-term instability of the power was less than 2%. The resonator was formed by a spherical total-reflection mirror with a radius of curvature of 1 m and by a diffraction grating (with a reflection coefficient of 0.9 in first order). The grating was set up in an autocollimation regime. The baseline of the resonator was 0.95 m, the length of the active medium was 0.35 m, and the diameter of the discharge tube was 8 mm. The active medium consisted of a CO_2:N_2:He = 1:1:5 gas mixture at a pressure of 27 torr. For the Q switching we used a refractive acoustooptic modulator with a KRS-5 crystal, positioned in the resonator at the Brewster angle. The modulator made it possible to produce a sinusoidal loss modulation in the frequency range 10–300 kHz at steps $\approx$10 kHz (Ref. 40). Additional studies of the characteristics of this modulator outside the resonator revealed that the modulation depth for this particular modulator was a linear function of the amplitude of the control voltage and reached 30% at a control signal of 50 V at a modulation frequency of 180 kHz.

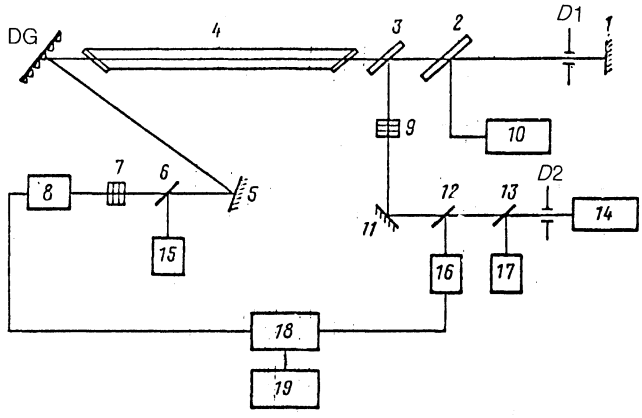

FIG. 1. Experimental layout. *1,5,11*—Mirrors; *D* 1,*D* 2—diaphragms; *2*—modulator; *3*—GaAs plate; *4*—discharge tube; DG—diffraction grating; *6,12,13*—beam splitters; *7*—attenuator; *8*—CdHgTe photodetector; *9*—neutral filters; *10*—G4-153 oscillator; *14*—Nd:YAG laser; *15,17*—IMO-2 energy and power meters; *16*—FK-15 photodetector; *18*—S9-8 oscilloscope; *19*—IBM PC/AT microcomputer.

The temporal characteristics of the output were studied with a CdHgTe photodetector with a time resolution of 50 ns and also an S9-8 storage oscilloscope. An output signal from the S9-8 was fed through an interface to an IBM PC/AT computer for analysis and storage. The signal discretization frequency was chosen to suit the frequency resolution required and the frequency of the control signal. This discretization frequency could be varied up to 20 MHz. The total number of points was limited to 2048 by the amount of memory in the oscilloscope which we used. In finding the spectra of the signals of interest from these points, we eliminated the constant components and the slowly varying components which were unrelated to the useful signal.

In-resonator amplitude modulation of the light intensity of a cw CO_2 laser was proposed in Refs. 41 and 42 and implemented here. The modulation in that case resulted from an optically controllable absorption at nonequilibrium charge carriers in semiconductors excited in an intrinsic or extrinsic absorption band. The duration of the pulsed loss which was introduced was set by the length of the excitation pulse and by the lifetime of the nonequilibrium carriers in the semiconductors. For example, when a ZnSe plate was used as a modulator, and the beam from a ruby laser was applied to it, the duration of the loss which was introduced was $\leqslant$50 ns, no greater than the duration of the excitation pulse.

This method was used to shape short loss pulses in experiments on the small-signal gain near the threshold for period doubling and to study the possibility of switching between modulation regimes. For this purpose, we also installed a GaAs plate 2.8 mm thick in the resonator, at the Brewster angle, and we applied 15-ns pulses from a neodymium laser to it. The pulse energy was varied by means of a set of calibrated neutral filters. The decay time of the induced loss was estimated from the duration of the response by the method proposed in Refs. 43–45. It turned out to be about

300–400 ns and thus considerably shorter than the loss modulation period.

The same method for introducing a pulsed loss was used to determine the relaxation frequency ω_{rel} of the intensity oscillations of the output from the cw CO_2 laser and the dissipation coefficient γ. From these measurements we found $\omega_{rel} = 855 \pm 30$ kHz and $\gamma = 790 \pm 30$ kHz.

2. MULTIRESONANCE STRUCTURE IN THE NONLINEAR RESPONSE; TRANSITION TO CHAOS

The rate equations for a Q-switched laser can be written in the two-level model as[4,15,16]

$$\ddot{x}+(\varepsilon_1+\varepsilon_2 e^x)\dot{x}+(1+q\cos mt)e^x-1 = (qm/\varepsilon_2)\sin mt-(q\varepsilon_1/\varepsilon_2)\cos mt, \quad (1)$$

where x is the intensity on a logarithmic scale, q is the relative depth of the loss modulation $m = \omega_M/\omega_0$, ω_M is the modulation frequency, $\omega_0 = (\omega_{rel})^2 + \gamma^2/4)^{1/2} \approx 900 \pm 30$ kHz, and ε_1 and ε_2 are determined by the lifetime of photons in the resonator, by the relaxation of the population difference, and by the relative extent to which the pump exceeded the threshold. More complex models for the CO_2 laser, in particular, models which incorporate relaxation within the vibrational-rotational band, can also be put in the form of (1), through the use of the central-manifold theorem.[46] The physical interpretation of the results on experiments on modulation of the parameters thus reduces to an examination of forced oscillations of a nonlinear oscillator of the form (1).

The Toda potential $U(x) = \exp(x) - x$ is a "soft" potential, by which we mean that the frequency $\omega_0(a)$ of the free oscillations decreases with increasing oscillation amplitude a. Correspondingly, the peak on the resonance curves shifts to the left. In addition to the main resonance at $\omega_M \approx \omega_0(a)$, a nonlinear system can have secondary resonances at $\omega_M = \omega_0(a)k/l$, where k and l are relatively prime numbers. Corresponding to each of these resonances on the amplitude-frequency characteristic is a separate branch with a period of $2\pi/\omega_M$. The resonances at ultraharmonics ($\omega_M = \omega_0(a)/l$) appear in a process which does not involve a threshold, while the other resonances, in particular, those at subharmonics ($\omega_M = k\omega_0(a)$), are excited in a "hard" fashion. The height of the threshold is proportional to the dissipation coefficient $\varepsilon_1 + \varepsilon_2$ (Refs. 16 and 17). The overall picture of the sequence of appearance of resonances in the (q,m) plane is rather complicated. The results of numerical[20] and analog[22] modeling indicate that this sequence can be described by appealing to mathematical concepts from graph theory, in particular, the Farey tree.

The natural resonances of the modulator crystal at frequencies which are multiples of $v/2L$, where v is the velocity of sound and L is the length of the crystal, introduce difficulties in efforts to continuously tune the frequency with a fixed effective modulation amplitude. It is thus not possible to use direct methods to determine the experimental amplitude-frequency characteristic. Since the Toda potential is soft, however, various resonances can be observed by fixing the modulation frequency and increasing the modulation amplitude, as is illustrated in Figs. 2 and 3, respectively, for frequencies below and above the relaxation frequency. Figure 2 shows a sequence of regimes which starts from a sinusoidal regime and runs to regimes near resonances at the ultraharmonics 1/4, 1/3, 1/2, and 1/1. Characteristic features of the $1/n$ resonance are a fine structure in the trailing edges of the generation pulses, with a period of about $2\pi/\omega_M n$ and a nonmonotonic behavior of the envelope signal near ultraharmonic the n which is more prominent than the neighboring harmonics, by virtue of the resonance.

Note that the shortest period among all the regimes in Fig. 2 is $T_M = 2\pi/\omega_M$. There is no chaos even at fairly high values of the control voltage on the modulator. This result agrees well with the theoretical results of Refs. 16 and 17 and with the bifurcation diagrams shown there. Nevertheless, at fixed values of $\omega_M < \omega_0(a)$ and sufficiently large values of q we observed some narrow period-doubling zones as we smoothly varied one of the parameters (the discharge current or the unperturbed loss). Analysis of the intensity spectra in these regions indicates 2/3 and 2/5 resonances.

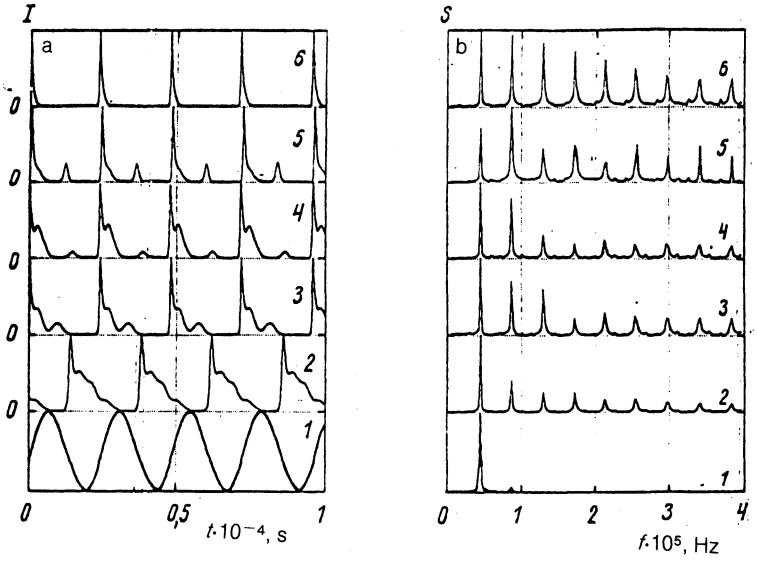

FIG. 2. a: Time evolution of the intensity of the laser output, $I(t)$. b: Corresponding spectra of the signals $S(f)$ at the modulation frequency $f_M = f_0/4$ for various values of the control voltage on the modulator. *1*–7 V; *2*—50; *3*—70; *4*—75; *5*—97; *6*—147 V.

The minimum thresholds for the appearance of a chain of period doublings, chaos, and resonance subharmonics occur near modulation frequencies $m \approx 1.7$, as predicted by the theory of Ref. 17. Figure 3 shows one example of a sequence of regimes observed in this case. The first period-doubling bifurcation arises as early as $V = 1.7$ V (for clarity, the regime of a well-developed period doubling at $V = 2.25$ V is shown on line 2). This regime then becomes a resonance regime (line 3). The subharmonic $\omega_M/2$ dominates the spectrum. The shape of the spectrum and the shape of the intensity oscillations are essentially the same as in the case of the main resonance (line 6 in Fig. 2). With a further increase in modulation depth, we find a cascade of period doublings, which terminates in chaos (line 5 in Fig. 3). The high signal-to-noise ratio in our experimental apparatus made it possible to stably observe regimes with periods up to $16T_M$ and to find an experimental estimate of the universal Feigenbaum scaling constant, $\delta_F \approx 4.4$. One reason for the deviations of this estimate from the exact value $\delta_F = 4.669$ is the nonlinearity of the function $q(V)$.

Chaos of the type shown on line 5 in Fig. 3 exists in the interval $V = 6.2$–7.0 V. The strange attractor undergoes several internal restructurings in this interval, as a consequence of successive collisions with unstable cycles. This "inverse" cascade of internal bifurcations is typical of systems which exhibit a transition to chaos through period doubling.[26,27] We observed the last stage of this process. A characteristic feature of the spectra averaged over many realizations in this case is the presence, against the continuous background, of discrete components at the frequencies $nm/4$, $n = 1,2,3,\ldots$. In this case the dynamic chaos is reminiscent of a "noisy" periodic regime with a period of $4T_M$. At $V = 7.0$ V, the last event of the chain of internal crises occurs. It is caused by a collision (in phase space) of a strange attractor and an unstable cycle with a period of $2T_M$ (Ref. 19). The topological structure and the spectrum (Fig. 3, b and c, line 6) change sharply. In particular, the discrete components of the frequencies $nm/4$, $n = 1,2,3,\ldots$, disappear from the spectrum. In this sense the signal becomes more chaotic.

At $V = 7.25$ V, this strange attractor disappears through a crisis of boundaries upon a collision with an unstable saddle cycle with a period of $3T_M$, which gives way to a stable subharmonic regime with a period of $3T_M$ (line 7 in Fig. 3). We wish to stress that the latter regime is the subharmonic 3/1 branch, not the usual periodic window within a chaos, as has been seen previously.[16,17,26,27] When the control voltage on the modulator is scanned in the opposite direction, a hop from this branch is observed at $V = 5.5$ V. This result implies generalized bistability (in the sense of Ref. 25) in this interval of the control parameter. In other words, the implication is that modulation regimes coexist which differ in not only the amplitude but also the period and the nature of the modulation (chaotic or regular).

At control voltages up to values corresponding to the regime with a period of $3T_M$, the average laser output power remains essentially constant (at ≈ 0.24 W). The implication is that the pulsed power increases by a factor of 5–15, depending on the modulation regime. With a further increase in the control voltage, the average power decreases, and at sufficiently high voltages ($V \approx 45$ V) the lasing is cut off.

3. STATISTICAL PROPERTIES OF THE CHAOS

The results in Sec. 2 are sufficient but still indirect proof that the chaos is of a dynamic nature. There are direct diagnostic methods which can work from a single experimental realization. These methods are based on ergodic theory.[47] In particular, these methods can provide estimates of the frac-

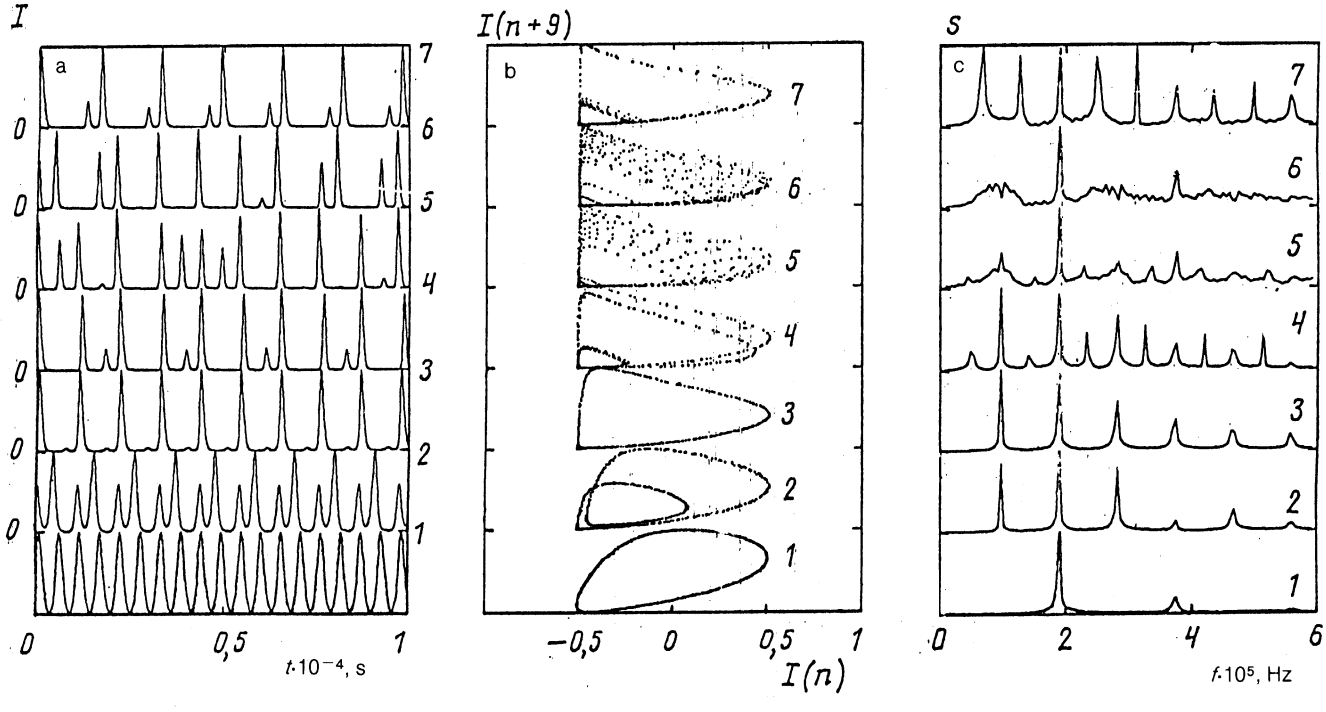

FIG. 3. a: Time evolution of the laser output intensity, $I(t)$. b: Reconstructed phase portraits $[I(n+9), I(n)]$. c: Signal spectra at the modulation frequency $f_M \approx 1.4 f_0$ for several values of the control voltage on the modulator. *1*—1 V; *2*—2.25; *3*—4; *4*—5.7; *5*—6.5; *6*—7; *7*–8 V.

tal dimension of the strange attractor and the Kolmogorov entropy.[48] A positive and finite value of this entropy means that there is at least one positive Lyapunov exponent. A positive and finite Kolmogorov entropy is also the strongest criterion for a dynamic stochastic nature and the criterion most frequently used.

Low-dimension strange attractors were found in the very first experimental studies of quantitative characteristics. These were studies of an He–Xe laser with an inhomogeneously broadened line[49] and of a CO_2 laser with an electrooptic loss modulator.[50] The fractal dimension of a strange attractor in a He–Ne ring laser with oppositely directed waves, with a periodic modulation of the frequency "support," was recently measured experimentally. A foundation was thus laid for a phenomenological model for such lasers, with a phase space smaller than that for the Lamb system of equations.[51]

There is heuristic value in finding such invariants of strange attractors as their dimension: The effective number of degrees of freedom which are involved in the dynamics can be determined directly, so it becomes possible to construct or refine a theoretical model of the system.

Our purpose in the present section of the paper is to study the quantitative characteristics of the dynamic chaos in a CO_2 laser with an acoustooptic loss modulator in both the single-mode regime (Sec. 2) and the multimode regime (in terms of the transverse index). In contrast with previous studies, we also examine the effect of preliminary filtering of the signal. Here is an overall outline of studies of this sort.

The first step is to reconstruct a phase portrait in an M-dimensional imbedding space on the basis of one discrete experimental realization $I(i\Delta t_d)$, where Δt_d is the sampling interval, and $i = 1,2,3,\ldots, n$. Here we use the rule proposed by Takens:[52]

$$\{y_j\}=\{I_j, I_{j+1}, \ldots, I_{j+M-1}\}, \tag{2}$$

where $\{y_j\}$ is a state vector in the M-dimensional space, and r is the distance between points in this space.

Figure 3b shows examples of such a reconstruction for $M = 2$. The next step is to calculate the generalized correlation sum[51]

$$C_s^{(M)}(r)=\left\{\frac{1}{N_M}\sum_i\left[\frac{1}{N_M}\sum_j H(r-\|y_i-y_j\|)\right]^{(s-1)}\right\}^{1/(s-1)}, \tag{3}$$

where N_M is the number of points in the reconstructed attractor, $H(r) = (1 + \operatorname{sgn} r)/2$ is the unit step function, and $\|y_i - y_j\|$ is any of the known norms. Particularly convenient in practice is the norm

$$\|y_i-y_j\|=\max |I_{i+k}-I_{j+k}|,\ k=0, 1, \ldots, M-1.$$

In this case the numerical algorithm for calculating the quantity in (3) simplifies dramatically. In the important particular case of a correlation dimension ($s = 2$), which is the one used most frequently in practical calculations, the algorithm can be implemented in integer numbers.[53] In addition, the following relation holds in this case:[54]

$$\lim_{\substack{r\to 0,\ N_M\to\infty,\\ M\to\infty}} \ln C_s^{(M)}(r) = D_s \ln r - M\Delta t_3 K_s + \text{const}, \tag{4}$$

where D_s and K_s are the generalized dimension and generalized entropy, respectively, of order s. As can be seen from (4), the slope of the linear part of the plot of $C_s^{(M)}(r)$ in double logarithmic scale is D_s, and the quantity proportional to the entropy is

$$\Delta t_3 K_3 = \lim_{M\to\infty} \ln[C_s^{(M)}(r^*)/C_s^{(M+1)}(r^*)], \tag{5}$$

where r^* is chosen in the region of linear scaling. The spectrum of generalized dimensions of uniform fractals such as the von Koch curve and the Serpinskiĭ carpet is uniform: $D_{s+1} \equiv D_s = D_0$, where the dimension D_0, the capacity, is determined exclusively by the metric of the fractal.[47] Actually, we are dealing with multifractals, with different values of D_s and with $D_{s+1} < D_s$. It follows that the correlation dimension D_2, the simplest to calculate, is a lower estimate of the capacity D_0 of a strange attractor and of the dimension D_1, called the "information dimension."[47] The estimate becomes more accurate as the strange attractor becomes more uniform. Correspondingly, the correlation entropy is a lower estimate of the Kolmogorov entropy K_1: $K_2 \leqslant K_1$. For moderately nonuniform fractals, the differences between D_2 and K_2 (on the one hand) and D_0 and K_1 (on the other) are usually no more than a few percent.

The specific calculations had to be restricted to finite values of r, N_M, and M. The arbitrariness in the choice of discretization interval Δt_d, the noise, the low accuracy of the analog-to-digital conversion, and the preliminary filtering may lead to systematic errors in the estimates of D_s and K_s (particularly for $|s| \gg 1$). The effects of these factors are discussed in detail in Ref. 55.

Our experimental apparatus was capable of storing a signal sample 2048 points long at a resolution of 8 bits (this resolution introduces an error of less than 5%; Ref. 55). The optimum delay Δt_d was chosen on the order of the first zero of the autocorrelation function and then corrected, in the direction of decreasing value, on the basis of the empirical condition that the final result remain unchanged. In this fashion we found the interval of optimum values to be $\Delta t_d = T_M/(8\text{–}16)$, in agreement with the results found on other systems with modulated parameters.[50,51,53]

A distinctive feature of loss-modulated lasers is that the reconstruction of the phase portrait from the temporal realization of the intensity, which is clearly of a peak nature, serves as a source of errors. Because of the large regions in which the intensity is essentially zero, most of the points of the reconstructed attractor also are bunched near zero. The nonuniformity of such an attractor is of course very high ($D_2 \ll D_0$). In particular, for a random signal of a quasi-two-level nature we would have $D_2 \approx 0$. In this case the value of D_2 essentially does not reflect the geometric structure of the attractor.

To get around this obstacle, we used preliminary filtering of the signal. Causal filtering (in real time, for example) introduces an extra degree of freedom and introduces a bias in the estimate of the fractal dimension.[56–58] We accordingly used a code implementation of a noncausal filter with the real transfer characteristic

$$H(\omega)=1/(1+\alpha|\omega|^p), \tag{6}$$

where α and p are chosen in such a way that the fine structure

in the signal is retained. By varying α at a given p, we can determine the optimum value α_{opt}, i.e.., that which maximizes D_2.

Figure 4a shows the correlation sum $C_2^{(M)}(r)$ for the chaotic regime shown on line 5 in Fig. 3. We can distinguish three basic regions on these plots: $6.5 \leqslant \log_2 r < 8$, $5 \leqslant \log_2 r < 6.5$, and $\log_2 r \leqslant 5$. Only the central interval, the "scaling region," is informative. The slope of the first region is determined by boundary effects, and that of the third by noise and the inadequate statistical base.

Figure 4b shows $D_2(M)$ found by linear regression in the scaling zone for various conditions in the preliminary processing of the data. In the case of curve *2* there was no filtering; curve *3* corresponds to the case of the optimum filter with $p = 1$, we have $\alpha_{opt} = 10^{-2}$); curve *4* shows the logarithm of the signal; and curve *5* shows a combination of the preceding operations. We see from this figure that curves *2–5* all have saturation regions for $M \geqslant 17$, where $D_2 \approx 2.2$ (if we ignore the slight increase due to the noise). An optimum filtering improves the estimate by about 5%. It is also useful to take the logarithm of the filtered signal. In this case we find a satisfactory estimate of the dimension even for $M \geqslant 7$. This result agrees with the Mañé theorem, that it is possible to adequately reconstruct an attractor of dimension D_2 in an embedding space with $M \geqslant 2D_2 + 1$ (Ref. 59).

The random error in the determination of D_2 by linear regression in the scaling region is extremely small. Consequently, the overall error in the measurements of D_2 is determined primarily by the systematic errors caused by the finite precision of the analog-to-digital conversion and by the noise;[55] these components of the error are opposite in sign. On the basis of the discussion above we can assume $D_2 = 2.2 \pm 0.1$ in the single-mode regime.

Also shown in Fig. 4b are results calculated on $D_2(M)$ for a periodic regime (curve *1*) and for a multimode regime (curve 6), in terms of the transverse index. In the former case we are dealing with a limit cycle—a closed line in phase space—so we have $D_2 \approx 1.0$ even for $M \geqslant 3$. In the multimode case (the number of modes was not monitored), the $D_2(M)$ curve does not reach saturation. It instead rises monotonically with increasing M. There are several possible reasons here. First, the sample length ($N_M = 2048$) is generally too short for successful reconstruction of a high-dimension attractor (according to estimates in Refs. 60 and 61, the minimum number sufficient is $N_M \geqslant 42^{D_2}$). Second, multimode generation may be time-varying because (in particular) the loss modulation depths are sharply different for the different modes in the acoustooptic modulator. This circumstance may lead to a complex picture of switching between attractors with different dimensions, disruptions of the signal phase, and smearing of a reconstructed attractor in the phase space.

Figure 4 shows the quantity $F_2 = K_2 \Delta t_3 / \ln 2$ as a function of the dimension M of the embedding space for regular and chaotic single-mode regimes. For the periodic regime we have $K_2 = K \equiv 0$. In the chaotic regime we have $K_2 \approx 76 \pm 5$ kHz. The error was found as the deviation from the mean value for r^* from the scaling zone.

Similar calculations carried out for a strange attractor after an internal crisis (line 6 in Fig. 3) showed that the dimension D_2 remains essentially the same, while K_2 increases slightly.

Here is a physical interpretation of the results. The chaotic oscillations observed in the laser intensity are actually of a dynamic nature ($K_2 > 0$). The processes which occur in a single-mode laser can be described by using nonautonomous rate equations with a three-dimensional phase space ($D_2 < 3$).

In a three-dimensional phase space, a dynamic system has three Lyapunov exponents. The leading exponents are $\lambda_1 \geqslant K_2$, $\lambda_2 = 0$, and $\lambda_3 = -\gamma - \lambda_1$, where γ is the dissipation coefficient in the system. Independent measurements of γ from the damping of small free oscillations in the laser output intensity yield $\gamma = 790 \pm 30$ kHz. We thus find $\lambda_3 \leqslant -860$ kHz. On the basis of these results we can estimate the Lyapunov dimension of the attractor: $D_L = 2 + \lambda_1/|\lambda_3| \approx 2.1 \pm 0.05$. Within the errors, this result is the same as the correlation result. A similar relation between these quantities was observed in Ref. 18 in a numerical simulation of the rate equations (1).

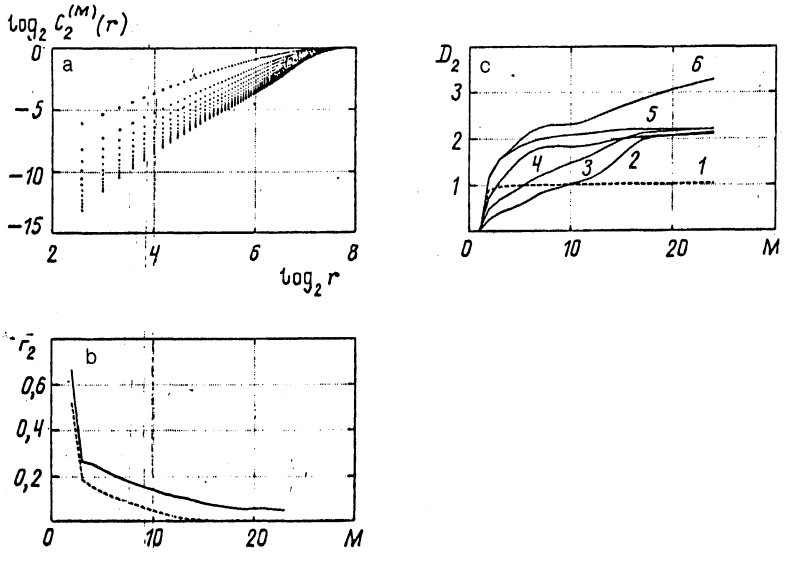

FIG. 4. a: The correlation integral $C_2^{(M)}$ versus r in double logarithmic scale for the chaotic regime (line 5 in Fig. 3) and for imbedding spaces with $M = 2, 4, \ldots, 12$. b: Slope of the curve of $\log_2 C^{(M)}(r)$ versus $\log_2 r$ in the scaling zone as a function of M. *1*—Regular regime (line 1 in Fig. 3); *2–5*—chaos (line 5 in Fig. 3) for various types of preliminary analysis of the data (see the text proper for an explanation). c: Normalized correlation entropy $F_2 = K_2 \Delta t_3 / \ln 2$ as a function of M for the regular regime (dashed line, delay time $\Delta t_d = 200$ ns) and for the chaotic regime (solid lines, $\Delta t_d = 500$ ns).

4. SMALL-SIGNAL GAIN NEAR A PERIOD-DOUBLING BIFURCATION

We consider a composite perturbation of the loss in the laser resonator, consisting of a harmonic part and a brief pulsed part, at the time t_0. Equation (1) is modified in the following way:

$$\ddot{x}+[\varepsilon_1+\varepsilon_2\exp(x)]\dot{x}+(1+q\cos mt)\times\exp(x)-1=(qm/\varepsilon_2)\sin mt-(q\varepsilon_1/\varepsilon_2)\cos mt-(q_0/\varepsilon_2)\dot{\delta}(t-t_0)-(q_0/\varepsilon_2)\{\varepsilon_1+\varepsilon_2\exp[x_0(t_0)]\}\delta(t-t_0), \quad (7)$$

where $\delta(t-t_0)$ is the Dirac δ-function. In the limit $q_0 \ll q$, we have the following equation for the case of a small deviation of $\zeta(t)$ from a steady-state periodic solution $x_0(t)$:

$$\ddot{\xi}+[\varepsilon_1+\varepsilon_2\exp(x_0)]\xi+[1+q\cos(mt)+\varepsilon_2\dot{x}_0]\exp(x_0)\xi=-(q_0/\varepsilon_2)\dot{\delta}(t-t_0)-(q_0/\varepsilon_2)\{\varepsilon_1+\varepsilon_2\exp[x_0(t_0)]\}\delta(t-t_0). \quad (8)$$

The function $\zeta(t)$ is zero except at $t>t_0$. It is the response to a $\delta(t)$ perturbation of a linear system with coefficients which are periodic in time. The physical interpretation of the amplification effect is based on a parametric mechanism for a period-doubling bifurcation.[16] System (8) is a parametric amplifier with a self-pumping period $2\pi/\omega_0'$ which is equal to the period of the function $x_0(t)$. From the continuous spectrum of the δ-function, the parametric amplifier selectively passes only those frequencies which lie near $l\omega_0'/2$, $l=1, 3, 5, \ldots$. In particular, in the case of a monochromatic pump with an amplitude A the transmission coefficient H, averaged over the period $2\pi/\omega_0'$, is[62]

$$H^2\equiv\langle|K(\omega, t)|^2\rangle\propto 1/(\Delta^2+\alpha^2\varepsilon^2), \quad (9)$$

where $\Delta=\omega-l\omega_0/2$, l is odd, $\alpha=(\varepsilon_1+\varepsilon_2)/2$, and the parameter $\varepsilon=1-|A|/|A_{\text{thr}}$ characterizes the distance of the system from the period-doubling threshold.

The same result can be found by a more formal method. Specifically, the nonautonomous equation (8) is equivalent to an equation with initial conditions:

$$\ddot{\xi}+\{\varepsilon_1+\varepsilon_2\exp[x_0(t+t_0)]\}\dot{\xi}+\{1+q\cos[m(t+t_0)]+\varepsilon_2\dot{x}_0(t+t_0)\}\exp[x_0(t+t_0)]\xi=0,$$
$$\xi(t=+0)=-q_0/\varepsilon_2, \quad \dot{\xi}(t=+0)=0, \quad (10)$$

where we have made the substitution $t\to t_0+t$. The effect of a brief change in the loss thus reduces to an instantaneous decrease in the intensity by a factor of $\exp(-q_0/\varepsilon_2)$. According to the Floquet theorem, a general solution of Eq. (10) is

$$\xi=\xi_1+\xi_2=C_1\exp[-\alpha(1-\mu/\alpha)t]\varphi(t, \sigma_1)+C_2\exp[-\alpha(1+\mu/\alpha)t]\varphi(t, \sigma_2), \quad (11)$$

where the constants C_1 and C_2 are determined by the initial conditions. The function $\varphi(t,\sigma)$ has a period $4\pi/\omega_0'$. Its spectrum has no components at frequencies which are multiples of ω_0. This function, along with the growth rate μ and the parameters $\sigma_{1,2}$, can be calculated analytically to arbitrary accuracy in the form of converging series, provided that we know the coefficients in the Fourier-series expansion of the function $x_0(t)$. The reason is that in this case Eq. (9) can be reduced to the canonical form of the generalized Hill equation.[17]

Near the bifurcation ($\varepsilon=1-\mu/\alpha\ll 1$) the first of the particular solutions, $\zeta_1(t)$, dominates the general solution. At the time, the short-lived solution $\zeta_2(t)$ is damped even more rapidly than in the case without modulation ($\mu=0$).

On the other hand, it is clear that this effect depends on the phase, i.e., on the time t_0 at which the δ-function perturbation is applied, through the parameters $\sigma_{1,2}$. There exist t_0' and t_0'', which are determined by

$$\dot{\varphi}(0, \sigma_2(t_0))-(\alpha+\mu)\varphi(0, \sigma_2(t_0))=0, \quad (12)$$
$$\dot{\varphi}(0, \sigma_1(t_0))-(\alpha-\mu)\varphi(0, \sigma_1(t_0))=0,$$

such that we have $C_1\equiv 0$ or $C_2\equiv 0$. In other words, there are directions in phase space along which there are fast and slow relaxations of perturbations from a given periodic regime. These directions depend on t_0. If $t=t_0''$ ($C_2=0$) holds, a deviation with an amplitude q_0/ε_2 lies entirely on the slow "central manifold,"[63] and the gain is a maximum. At

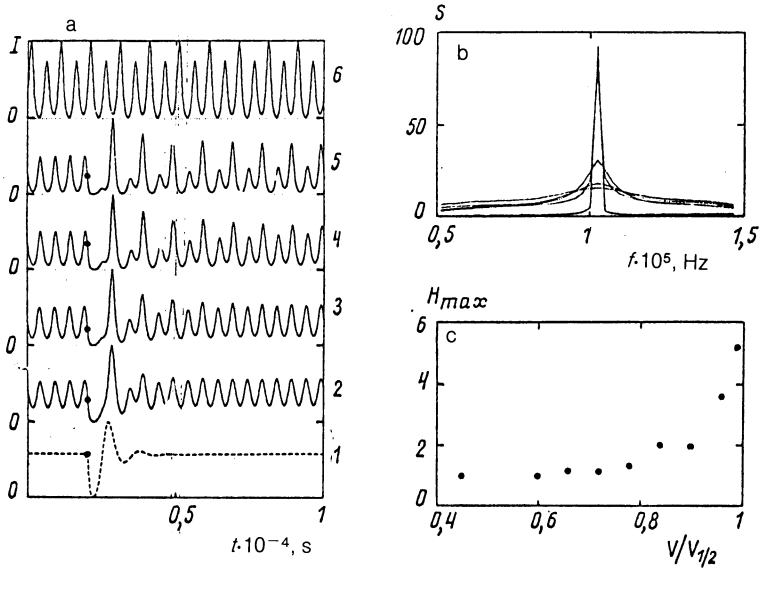

FIG. 5. Small-signal gain near a period-doubling bifurcation ($V_{1/2}=1.67$ V, $f_M\approx 200$ kHz, excitation energy $W\approx 0.25$ mJ/cm^2). a: Response of a laser to a brief perturbation of the loss at the time t_0 (marked, here and below, by the circle) at several values of the control voltage. *1*—$V=0$; *2*—$0.45V_{1/2}$; *3*—$0.66V_{1/2}$; *4*—$0.9V_{1/2}$; *5*—$0.98V_{1/2}$. *6*—Steady-state regime with a period of $2T_M$ for $V>V_{1/2}$. b: Transmission frequency band near $f_M/2$ for cases *2–5* in frame *a* of this figure. c: Maximum gain H_{max} as a function of a subcriticality parameter $V/V_{1/2}$.

$t = t_0''$ ($C_1 = 0$), the perturbation acts in a direction orthogonal to the central manifold, and the response of the laser is rapidly damped. If noise is applied to the system, the fluctuations will naturally stretch out in one direction and contract in another.

Experiments with a composite pulsed-plus-periodic modulation of the Q of the resonator of a CO_2 laser completely confirm the behavior described above. Figure 5a shows the response of a laser to a brief and small perturbation of the loss, as a function of the distance from the control voltage to the first period-doubling threshold. The energy of the pulse exciting the Nd:YAG laser was chosen to keep the response in the linear regime. Shown for comparison here are the response of the laser to a similar perturbation of the loss in the absence of modulation (line 1) and the time evolution of the intensity after period doubling (line 6). The fact that the intensity relaxes with a high accuracy (the error is less than 0.1%) to its steady-state value before a pulsed perturbation is evidence that aftereffects (the heating of the GaAs plate, the thermal expansion associated with this heating, the shift of the lasing frequency, etc.) are negligible.

We should add that the damping of the relaxation oscillations ($\gamma = 790 \pm 30$ kHz) is slightly more rapid than predicted by calculations based on independent experimental data, within the framework of the two-level model. Similar results were found in Ref. 64, in a study of the linear response of a CO_2 laser to a weak, periodic modulation of the resonator length. As was shown in Ref. 64, this contradiction can be resolved on the basis of more complex multilevel models for the CO_2 laser, in particular, with the help of the vibrational-rotational model which we mentioned in Sec. 2. Since any of these models can be thought of as an equation of motion for some effective nonlinear oscillation of the type in (1), with corresponding "friction" coefficients, these models would not alter the qualitative conclusions, and this circumstance is of no fundamental importance for the questions with which we are concerned here.

In Fig. 5a we see that as the period-doubling threshold is approached the laser becomes more sensitive to a pulsed perturbation. Figure 5b and c, shows the spectra of the response near half the modulation frequency and a plot of the maximum gain H_{max} versus the subcriticality parameter, respectively. In a first approximation, the gain line can be assumed to be approximately Lorentzian [see expression (9)]. As the critical value $V_{1/2} = 1.67$ V is approached, the gain increases, and the effective gain band $\Delta\omega_g$ shrinks. The product of $H_{max}^{1/2}$ and $\Delta\omega_g$ remains approximately constant. A similar picture is observed at frequencies $\omega = l\omega_M/2$, with l odd, and also near the thresholds for other doubling bifurcations.

The results above were obtained at a fixed value of the time t_0 of the pulsed perturbation with respect to the phase of the periodic-modulation signal. Figure 6 shows the phase dependence of the gain. All four cases here (a–d) correspond to the same experimental conditions, except the time t_0 at which the pulsed perturbation is applied (this time is marked by the circle). In case a we see the maximum response of the laser [the long-lived particular solution $\zeta(t)$ dominates the general solution]. In contrast, when the application time t_0 is shifted by about π/ω_M (Fig. 6b), the laser goes back to its original state essentially instantaneously (the particular solution ζ_1 is dominant). Intermediate cases are shown in frames c and d in Fig. 6.

No phase dependence of the small-signal gain near a period doubling was noted in previous studies.[38,39] It is shown here for the first time. When a random train of δ-function pulses (a fairly realistic model) is applied to a laser, we should evidently observe a classical compression of the noise.

The function $\zeta(t,t_0)$ described by expression (11) is the instrumental function of the system. In other words, by using this function one can calculate the response of a laser to an arbitrary perturbation of the loss $f(t)$, and one can also solve the inverse problem.

Near a period-doubling bifurcation, the amplitude of the response (with appropriate phase relations) may be larger by a factor of ε^{-1} than in conventional in-resonator measurement layouts.[35] Accordingly, this effect is extremely promising for use in increasing the sensitivity of such measurements.

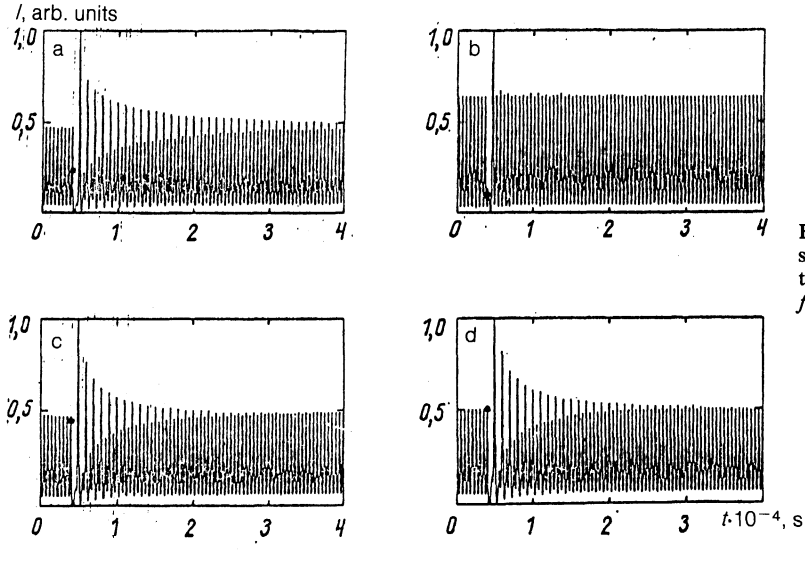

FIG. 6. Phase dependence of the response of a laser to a brief and small perturbation of the loss near a period-doubling bifurcation. The other parameters are the same for all of frames a–d: $f_M \approx 200$ kHz, $V = 2$ V, and $W \approx 0.55$ mJ/cm^2.

5. OPTICAL SWITCHING OF MODULATION REGIME; THE LASER AS AN AMPLITUDE VERSION OR PHASE VERSION OF AN OPTICAL FLIP-FLOP

In this section of the paper we report the results of an experimental study of optical switching of the modulation regime in a CO_2 laser. We find these results interesting primarily in connection with the effort to control the output characteristics of CO_2 lasers. From the standpoint of optical information processing, these results should of course be regarded as a possible exploitation of nonlinear dynamic effects.

In the preceding sections of this paper, and also in several papers by other investigators,[25-27] it has been demonstrated that the phase space of a laser with a modulated parameter is rather complex. Over wide ranges of the control parameters there may exist various modulation regimes (generalized multistability). Whether one regime or another is reached is determined by the initial conditions. Experimentally, this situation is usually reflected in hysteresis in the change in regime upon a smooth sweep of the control parameter.

An additional optically controllable pulsed perturbation of the resonator loss may be thought of as an equivalent change in the initial conditions when the pulse is applied. The imaging point jumps into a different region of the phase space. By the time the pulse ends the system may be in a basin of attraction to another attractor, so there will be an optical switching from one region to another. If the state of the system at the end of a pulse corresponds to a separatrix (a boundary separating the attraction of different attractors) or to an unstable cycle, then the system may spend a fairly long time in this unstable state before it switches to a new state or reverts to its old state, depending on the precision of the moves and also depending on the noise level. It is thus possible to experimentally determine the amplitude of an unstable cycle and—from a broader standpoint—to experimentally study the global phase portrait of the system.

We carried out some experiments on an apparatus with a composite periodic and pulsed modulation of the parameters, as described in Sec. 2. As the source of the optically controllable pulsed loss we used a GaAs plate, which was periodically exposed to pulses from a Q-switched Nd:YAG laser (the pulse length was ≈ 15 ns, and the repetition frequency 12.5 Hz). In contrast with the preceding section of this paper, where we were concerned with critical slowing regimes near a doubling bifurcation, the working range of the control voltage on the modulator was chosen at a fair distance from bifurcation points. In addition, since we do not need to require that the response be linear in this case (i.e., we do not need to require that the perturbation be small), we varied the energy of the pulses from the Nd:YAG laser over a broader range. The frequency of the voltage applied to the modulator was 200 kHz and was chosen in such a way that we achieved the richest bifurcation diagram (Sec. 2). By choosing the time at which the pulsed perturbation was applied—it is actually this time which determines the direction in which the imaging point moves in the Poincaré section with respect to the separatrices—we can easily control the switching regime. If the time at which the perturbation is applied is fixed, switching can be observed as the amplitude of the perturbation increases, i.e., as the energy of the pulse from the Nd laser increases.

Before we move on to a discussion of these results, we would like to point out that the concept of a generalized multistability includes not only an amplitude multistability (i.e., the case in which two coexisting modulation regimes belong to different resonant branches of the nonlinear response of the laser; these regimes may differ in modulation period) but also phase multistability. Let us explain. If a response with a period NT_M to an external modulation of frequency $\omega_M = 2\pi/T_M$ is observed in a laser, then it follows automatically that there are another $N-1$ regimes which are of exactly the same amplitude but which are shifted in phase by $2\pi/N$ with respect to each other. The reason is that these regimes are physically indistinguishable with respect to the modulation signal. The situation here is extremely similar to the processes which operate in parametric subharmonic generators in the rf range (parametrons), which were studied intensely in the late 1950s and the early 1960s as devices exhibiting discrete values of the phase of stable oscillations.[65]

It follows that after the first period doubling two regimes coexist with a relative phase shift of π and a period of $2T_M$. Moreover, there is an unstable regime with a period of T_M. After the second doubling, there are four regimes, with a phase shift $\pi/4$ (and so forth).

We have observed this behavior experimentally. Figure 7 shows examples of phase switching with an intermediate excursion to an unstable cycle. In cases a and b, the laser was initially operating in a regime with a period of $2T_M$. In the first case, the laser spent more than 50 μs ($\approx 10T_M$) on an unstable T_M cycle after the application of the pulsed perturbation. It then returned to its original state (the phase shift between the final and initial states is zero, as is easily verified with the help of the $2T_M$-periodic reference signal shown by the dashed line).

In case b, in contrast, after a few briefer interludes on an unstable T_M cycle (the fact that these interludes are briefer is evidence that the separatrix has not been reached as precisely), the laser switches to a $2T_M$ periodic regime with a phase shift of π with respect to the original regime.

Figure 7, c and d, shows corresponding results in the case in which the initial state of the laser is a $4T_M$-periodic regime. The number of stable phase states doubles in this case: We observe switching with phase shifts of $3\pi/2$, π, and $\pi/2$ (the particular examples shown in Fig. 7, c and d, correspond to a phase shift of $\pi/2$). Moreover, at the modulation depths corresponding to Fig. 7d an amplitude bistability appears, as can be seen from the transition regime with a period of $3T_M$, which indicates proximity of an unstable cycle with the same period.

We wish to stress that the results in Fig. 7 are primarily a demonstration that it is possible to experimentally observe unstable cycles. From the standpoint of the switching times between regimes with a discrete phase state, it is clear that these results are quite the opposite of optimum results. Specifically, by varying the amplitude or time of application of the perturbation (Fig. 7, a and b), we observe switching times which are limited essentially by the duration of one modulation period. It is also pertinent to note here that the phase dependence of the time of the transitional period indicates that aftereffects of the pulsed perturbation of the loss

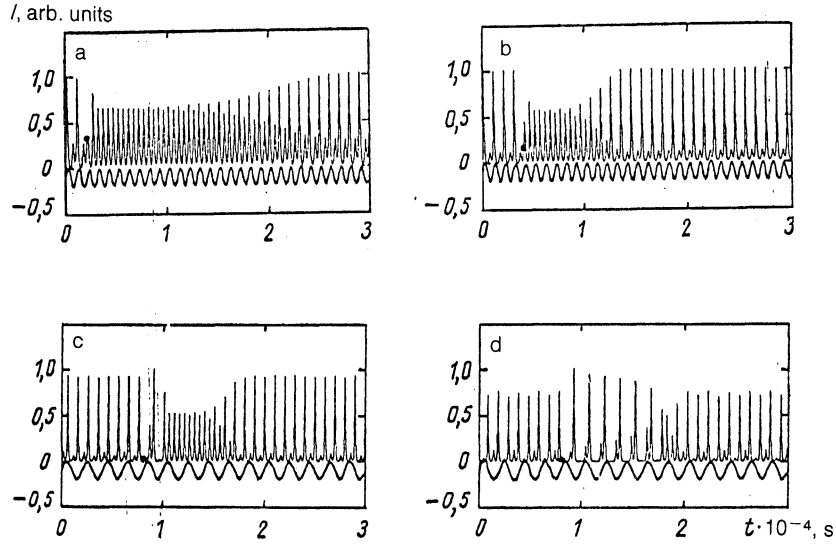

FIG. 7. Optical discrete switching of the phase of the modulation of a laser with an intermediate excursion to an unstable cycle. The dashed line shows a $2T_M$-periodic reference signal (in frames a and b) or a $4T_M$-periodic reference signal (in frames c and d). Here $f_M \approx 200$ kHz and $W \approx 0.25$ mJ/cm^2. a—$V = 2.03$ V; b—3.11; c—5.04; d—5.57 V.

are not playing an important role (at least at these energies of the exciting pulses).

Figure 8 shows the results of optical switching in which the final regime differs from the initial regime in both period and amplitude of the modulation. Frame a corresponds to a region of bistability between the 2/1 and 3/1 resonant branches. In contrast with Fig. 7d stable switching is achieved here; it is observed for hundreds of milliseconds. In addition, by repeating the pulsed perturbation we observe the opposite switching of regime, $3T_M \rightarrow 4T_M$.

Slightly more difficult to interpret are the results in Fig. 8b. The $4T_M$ periodic regime does not differ in amplitude from the original $2T_M$-periodic regime to the extent that we could say that there was a stable switching to a different resonant branch. At this energy of the excitation pulse (which was higher than that in the preceding cases by a factor ≈ 100), the effect of this pulse apparently does not reduce simply to a corresponding change in initial conditions. Instead, it also causes a brief change in the parameters, as can be seen in a shift of deformation of the entire bifurcation diagram. Further evidence for this interpretation comes from the fact that, after the brief perturbation of the loss, a phase with essentially no generation appears in the laser output and lasts for a fairly long time ($\approx 4T_M$).

We wish to stress that these results do not exhaust all possibilities in terms of a switching between regimes in a modulated laser. In particular, we observed stable switching between T_M-periodic generation regimes of different amplitude in the region of the main resonance.

In reviewing the results of this section of the paper, we note that we have demonstrated the rich possibilities for optical control of the output characteristics of CO_2 lasers with modulated parameters. In particular, we have demonstrated the operation of a modulated CO_2 laser as a binary phase flip-flop, a quadratic phase flip-flop, and an amplitude flip-flop (all of these being optical devices). These results may find applications in laser apparatus which requires rapid, reliable, and controllable switching of the repetition period

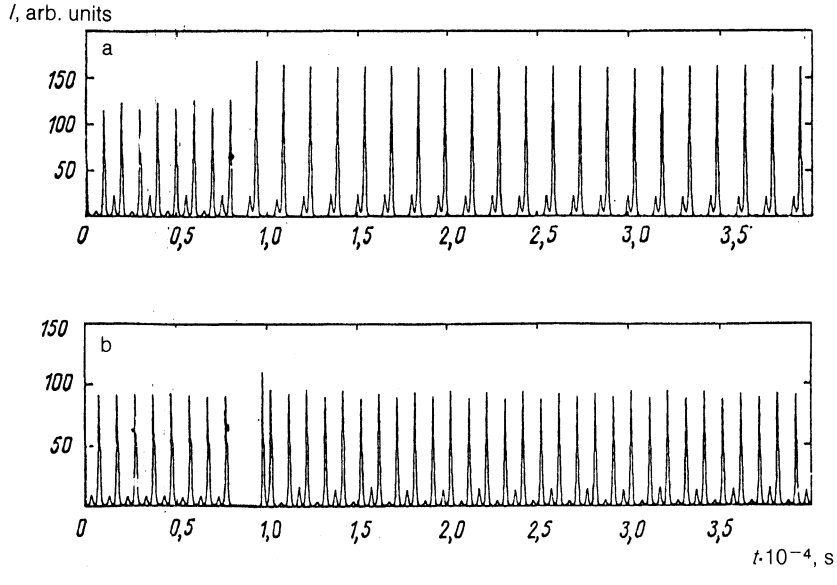

FIG. 8. Optical amplitude switching of modulation regime. a—$4T_M \rightarrow 3T_M$ ($f_M \approx 200$ kHz, $W \approx 0.25$ mJ/cm^2, $V = 5.5$ V); b—$2T_M \rightarrow 4T_M$ ($f_M \approx 200$ kHz, $W \approx 25$ mJ/cm^2. $V = 3.5$ V).

of the output pulses, the energy of these pulses, etc.

An extension of this idea (of combining a sinusoidal periodic modulation) of parameters with a pulsed modulation to the realm of semiconductor lasers and their applications may also be extremely promising for developing new instruments and apparatus. Finally, this method would be extremely useful for phase-space diagnostics in experiments on nonlinear dynamics in lasers.

CONCLUSION

We have carried out a detailed study of the resonance structure in the nonlinear response of a laser to a periodic modulation of the loss for various relations between the modulation frequency and the frequency of the relaxation oscillations. We have observed diverse temporal regimes in the lasing: from periodic trains of pulses which are greatly distorted by the presence of resonant ultraharmonics to random spiky lasing. In addition to the main resonance there are resonances at the relaxation frequencies 1/4, 1/3, 1/2, 2/3, 2/5, 2/1, and 3/1.

Working from experimental data on chaotic regimes, we have calculated the correlation dimension and the entropy for lasing regimes which are single-mode and multimode in terms of the transverse index. These results confirm that the chaos which is observed is of a dynamic nature. They also confirm that it is legitimate to use low-dimension theoretical models of the rate-equation type to describe such lasers. We have identified optimum conditions for a preliminary analysis of a peak signal on the basis of a suitable subsequent reconstruction of a phase portrait.

We have carried out a detailed study of the dynamics of a laser near a period-doubling bifurcation in the case of a combination of a sinusoidal modulation and a δ-function pulsed modulation of the resonator Q. We have demonstrated that there is a small-signal gain near frequencies which are multiples of half the modulation frequency. We have measured the gain and the frequency band as a function of a bifurcation parameter.

Experimentally, stable discrete switching of the phase and amplitude of the modulation has been achieved by means of a brief pulsed loss produced by means of an optically controllable in-resonator absorption of light in the semiconductor elements of a laser. We have observed that the initial phase of the modulating signal with respect to the pulsed loss affects the small-signal gain and the stability of the optical switching.

In summary, these experiments have demonstrated several new effects in lasers with modulated parameters. These new effects hold great promise for applications, in particular, in in-resonator kinetic measurements and in systems for optical information processing.

[1] K. Kubodera and K. Otsuka, IEEE J. Quant. Electron. **QE-17**, 1139 (1981).
[2] E. Brun, B. Derighetti, P. Meiser *et al.*, J. Opt. Soc. Am. B **2**, 156 (1985).
[3] M. M. Phillips, H. Gang, A. I. Ferguson, and D. C. Hanna, Opt. Commun. **61**, 215 (1987).
[4] É. M. Belenov, V. I. Morozov, and A. N. Oraevskiĭ, in *Quantum Electronics in Lasers and Masers*, Part 2 (Vol. 52, P. N. Lebedev Physics Institute Series), Trudy FIAN, 1970 (Consultants Bureau, New York, 1972).
[5] G. N. Vinokurov, Opt. Spectrosc. **31**, 472 (1971) [Opt. Spectrosc. (USSR) **31**, 251 (1971)].
[6] G. N. Vinokurov, N. M. Galaktionova, V. F. Egorov *et al.*, Zh. Eksp. Teor. Fiz. **60**, 489 (1970) [Sov. Phys. JETP **33**, 262 (1971)].
[7] V. A. Dement'ev, T. N. Zubarev, and A. N. Oraevskiĭ, in *P. N. Lebedev Institute Series*, Vol. 91, Trudy FIAN, 1979, p. 3.
[8] E. N. Lorenz, J. Atmos. Sci. **20**, 130 (1963); in *Strange Attractors* (Russ. Trans. Mir, Moscow, 1981, p. 88).
[9] A. N. Oraevskiĭ, in *P. N. Lebedev Institute Series*, Vol. 171, Trudy FIAN, 1986, p. 3.
[10] N. B. Abraham, P. Mandel, and L. M. Narducci, *Progress in Optics*, Vol. XXXV (ed. E. Wolf), Elsevier Sci., Amsterdam, 1988, p. 1.
[11] F. T. Arecchi, R. Meucci, G. Puccioni, and J. Tredicce, Phys. Rev. Lett. **49**, 1217 (1982).
[12] D. V. Ivanov, Ya. I. Khanin, I. I. Matorin, and A. S. Pikovsky, Phys. Lett. A **89**, 229 (1982).
[13] P. A. Khandokhin and Ya. I. Khanin, Kvantovaya Elektron. (Moscow) **11**, 1483 (1984) [Sov. J. Quantum Electron. **14**,1004 (1984)].
[14] L. G. Bezaeva, L. N. Kaptsov, and I. Z. Sharipov, Kvantovaya Elecktron. (Moscow) **12**, 1743 (1985) [Sov.J. Quantum Electron. **15**, 1152 (1985)].
[15] I. I. Matorin, A. S. Pikovskiĭ, and Ya. I. Khanin, Kvantovaya Elektron. (Moscow) **11**, 2096 (1984) [Sov. J. Quantum Electron. **14**, 1401 (1984)].
[16] A. M. Samson and S. I. Turovets, Preprint No. 438, Institute of Physics, Academy of Sciences of the Belorussian SSR, Minsk, 1986.
[17] A. M. Samson and S. I. Turovets, Dokl. Akad. Nauk BSSR **31**, 888 (1987).
[18] A. M. Samson and S. I. Turovets, Zh. Prikl. Spektrosk. **48**, 384 (1988).
[19] H. G. Solari, E. Eschenazi, I. Gilmore, and J. R. Tridicce, Opt. Commun. **64**, 49 (1987).
[20] T. Kurz and W. Lauterborn, Phys. Rev. A **37**, 1029 (1988).
[21] I. B. Swartz, Phys. Lett. **126**, 411 (1968).
[22] M. James and F. Moss, J. Opt. Soc. Am. B **5**, 1121 (1988).
[23] J. R. Tredicce, N. B. Abraham, G. P. Puccioni, and F. T. Arrecchi, Opt. Commun. **55**, 131 (1985).
[24] H. Goswami and D. J. Biswas, Phys. Rev. A **36**, 975 (1987).
[25] J. R. Tredicce, F. T. Arrechi, G. P. Puccioni *et al.*, Phys. Rev. A **34**, 2073 (1986).
[26] R. Meucci, A. Poggi, F. T. Arecchi, and J. R. Tredicche, Opt. Commun. **65**, 151 (1988).
[27] D. Dongoisse, P. Glorieux, and D. Hennequin, Phys. Rev. A. **36**, 4775 (1987).
[28] A. F. Glova, S. N. Kozlov, V. V. Likhanskiĭ, and V. P. Yartsev, in *Abstracts, Sixth All-Union Conference on Laser Optics*, Leningrad, 1990, p. 169.
[29] H. G. Winful, Y. C. Chen, and J. M. Liu, Appl. Phys. Lett. **48**, 616 (1986).
[30] W. Skishe, H. R. Telle, and C. O. Weiss, Opt. Lett. **9**, 561 (1984).
[31] A. C. Maciel, P. Maly, and J. F. Ryan, Phys. Rev. A **39**, 5455 (1989).
[32] D. Derozier, S. Bielawski, and P. Glorieux, Opt. Commun. **83**, 97 (1991).
[33] Y. Hori, H. Serizawa, and H. Sato, J. Opt. Soc. Am. B **5**, 1128 (1988).
[34] A. M. Samson, Yu. A. Logvin, and S. I. Turovets, Izv. Vyssh. Uchebn. Zaved., Radiofiz. **33**, 49 (1990).
[35] A. A. Mak, O. A. Orlov, and V. I. Ustyugov, Kvantovaya Elektron. (Moscow) **9**, 2412 (1982) [Sov. J. Quantum Electron. **12**, 1574 (1982)].
[36] K. Wiesenfeld and B. McNamara, Phys. Rev. Lett. **55**, 13 (1985).
[37] B. Derighetti, M. Ravani, R. Stoop *et al.*, Phys Rev. Lett. **55**, 1746 (1985).
[38] B. Segard, I. Zemmouri, and B. Macke, Opt. Commun. **63**, 339 (1987).
[39] J. Y. Bigot, A. Daunois, and P. Mandel, Phys. Lett. A **123**, 123 (1987).
[40] K. V. Kozlov, G. A. Pashkevich, V. N. Chizhevskiĭ, and V. V. Churakov, Kvantovaya Elektron. (Moscow) **16**, 744 (1989) [Sov. J. Quantum Electron. **19**, 486 (1989)].
[41] B. F. Kuntsevich, A. N. Pisarchik, V. N. Chizhevskiĭ, and V. V. Churakov, Zh. Prikl. Spektrosk. **38**, 126 (1983).
[42] V. N. Chizhevskiĭ and V. V. Churakov, Zh. Prikl. Spektrosk. **43**, 917 (1985).
[43] V. N. Chizhevskiĭ, Preprint No. 430, Institute of Physics, Academy of Sciences of the Belorussian SSR, Minsk, 1986.
[44] V. N. Chizhevskiĭ, Preprint No. 475, Institute of Physics, Academy of Sciences of the Belorussian SSR, Minsk, 1987.
[45] V. V. Kulikov, V. N. Chizheveskiĭ, and V. V. Churakov, Zh. Prikl. Spektrosk. **50**, 465 (1989).
[46] G. L. Oppo, J. R. Tredicce, and L. M. Narducci, Opt. Commun. **69**, 393 (1989).
[47] J.-P. Eckmann and D. Ruelle, Rev. Mod. Phys. **57**, 617 (1985).
[48] H. G. Schuster, *Deterministic Chaos*, Physik Verlag, Weinhein, 1988.
[49] A. M. Albano, J. Abounadi, T. N. Chyba *et al.*, J. Opt. Soc. Am. B **2**, 47 (1985).

[50] G. Piccioni, A. Poggi, W. Gadomski *et al.*, Phys. Rev. Lett. **55**, 339 (1985).
[51] I. E. Zuikov, P. G. Krivitskii, A. M. Samson, and S. I. Turovets, Pis'ma Zh. Tekh. Fiz. **16**, 34 (1990) [Sov. Tech. Phys. Lett. **16**(10), 779 (1990)].
[52] F. Takens, Lect. Notes Math. **898**, 366 (1981).
[53] W. Lauterborn and J. Holzfuss, Phys. Lett. A **115**, 369 (1988).
[54] J. G. Caputo and P. Atten, Phys. Rev. A **35**, 1311 (1987).
[55] M. Moller, W. Lange, F. Mitschke *et al.*, Phys. Lett. A **138**, 176 (1989).
[56] R. Badii, G. Broggi, B. Dereghetti *et al.*, Phys. Rev. Lett. **60**, 979 (1988).
[57] A. Chennaoui, J. Liebler, and H. G. Schuster, J. Stat. Phys. **59**, 1311 (1980).
[58] F. Mitschke, Phys. Rev. A **41**, 1169 (1990).
[59] R. Mañé, Lect. Notes Math. **898**, 230 (1981).
[60] L. A. Smith, Phys. Lett. **133**, 283 (1988).
[61] A. Wolo and T. Bessair, Physica D **50**, 239 (1991).
[62] S. A. Akhmanov, Yu. E. D'yakov, and A. S. Chirkin, *Introduction to Statistical Radiophysics and Optics*, Nauka, Moscow, 1981.
[63] J. Guckenheimer and P. J. Holmes, *Nonlinear Oscillations, Dynamical Systems and Bifurcations of Vector-Fields*, Springer-Verlag, New York, 1983.
[64] J. Y. Gao, H. Z. Zhang, X. Z. Guo *et al.*, Phys. Rev.A **40**, 6339 (1989).
[65] S. A. Akhmanov and M. A. Vorontsov (editors), *New Physical Principles for Optical Information Processing*, Nauka, Moscow, 1990.

Translated by D. Parsons